Proc. Natl. Acad. Sci. USA
Vol. 93, pp. 12171–12176, October 1996
Biochemistry

Redesigning secondary structure to invert coenzyme specificity in isopropylmalate dehydrogenase

(protein engineering/specificity/NAD/NADP)

RIDONG CHEN, ANN GREER, AND ANTONY M. DEAN

Department of Biological Chemistry, The Chicago Medical School, North Chicago, IL 60064-3095

Communicated by Richard A. Lerner, The Scripps Research Institute, La Jolla, CA, July 29, 1996 (received for review April 24, 1996)

ABSTRACT **Rational engineering of enzymes involves introducing key amino acids guided by a knowledge of protein structure to effect a desirable change in function. To date, all successful attempts to change specificity have been limited to substituting individual amino acids within a protein fold. However, the infant field of protein engineering will only reach maturity when changes in function can be generated by rationally engineering secondary structures. Guided by x-ray crystal structures and molecular modeling, site-directed mutagenesis has been used to systematically invert the coenzyme specificity of *Thermus thermophilus* isopropylmalate dehydrogenase from a 100-fold preference for NAD to a 1000-fold preference for NADP. The engineered mutant, which is twice as active as wild type, contains four amino acid substitutions and an α-helix and loop that replaces the original β-turn. These results demonstrate that rational engineering of secondary structures to produce enzymes with novel properties is feasible.**

The nucleotide binding folds of dehydrogenases fall into two broad classes, those having the βαβαβ motif characteristic of the Rossmann fold (1), and those formed from four loops that are characteristic of the decarboxylating dehydrogenases (2). The strong preferences displayed toward NAD or NADP by members within both classes provide attractive model systems to understand the structural determinants of specificity. In several cases coenzyme preferences have been inverted successfully (3–5), and in so doing the determinants delineated. However, inverting the coenzyme specificity of *Thermus thermophilus* isopropylmalate dehydrogenase (IMDH), a decarboxylating dehydrogenase, presents a singular challenge. Comparisons with the highly divergent *Escherichia coli* isocitrate dehydrogenase (IDH) suggest that success critically depends on engineering secondary structures within the coenzyme binding site (6).

T. thermophilus IMDH and *E. coli* IDH share only 24% sequence identity (7), yet retain similar tertiary structures (8). IMDH displays a 100-fold preference for NAD, whereas IDH displays a 7000-fold preference for NADP (Table 1). A comparison of high resolution x-ray structures of both binary complexes (6) indicates that the principle contributions to coenzyme binding and specificity arise through interactions between the adenosine moieties and residues lining a pocket on the large domain of both enzymes. Specificity in IMDH is conferred by the rigidly conserved Asp-278 (IMDH numbering, Table 2), which forms a double H-bond with the 2′- and 3′-hydroxyls of the adenosine ribose of NAD (Fig. 1*A*). Preference toward NAD is probably further enhanced by Asp-278, repelling the negatively charged 2′-phosphate of NADP. H-bonds also form between the N2 and N6 of the adenine ring and the main chain amide and carbonyl of residue 286 at the back of the pocket (not shown). There are no interactions between the bound NAD and residues in the β-turn. In IDH, a valine replaces the Ala-285 in IMDH, forcing the adenine ring of NADP to shift, weakening the H-bond to the N2, and reducing affinity for the coenzyme. However, new interactions established to the 2′-phosphate compensate for the lost H-bond. Asp-278 is replaced by a rigidly conserved lysine in IDH (Fig. 1*A*, Table 2), which is disordered in the crystal structure perhaps because its flexibility allows it to interact with any of the three phosphates of bound NADP. Ser-226′ (the prime indicates the second subunit of the homodimer) and the conserved Ile-279 of IMDH are replaced by the rigidly conserved Arg-226′ and Tyr-279 in eubacterial IDHs (Table 2), where they form H-bonds to the 2′-phosphate. In addition, a β-turn in the coenzyme binding pocket of IMDH is replaced by an α-helix and loop in IDH. This allows two additional residues, Tyr-325 (IMDH numbering) and *395-Arg* (IDH numbering and italicized because it has no equivalent in the β-turn of IMDH) to H-bond with the 2′-phosphate (Fig. 1*A*). Clearly, maximizing interactions between the enzyme and the 2′-phosphate requires that the secondary structure of IMDH be engineered from a β-turn to an α-helix and loop.

MATERIALS AND METHODS

Molecular Modeling. A model of the NADP dependent mutant was constructed by introducing an IDH-like α-helix and loop together with the requisite substitutions into a model of IMDH in which the two domains had been superposed on those of the catalytically active conformation of IDH (25). A phosphate was added at the 2′ position of the NAD ribose and the resulting structure subjected to energy minimization using the CHARMM force field as implemented in QUANTA on a Silicon Graphics 4D120/GTX. Only the IDH-like α-helix and loop and the mutated residues were subjected to minimization for the first 50 steps, during which the N6 amine of the NADP adenine ring was also constrained to remain in its original position above the imidazole ring of His-273. Thereafter, all restraints, on the coenzyme, on amino acids contacting residues in the coenzyme binding pocket, on amino acids contacting residues in the engineered α-helix and loop, and all residues within 8 Å of the coenzyme were removed. The final 100 steps of 1000 steps of minimization reduced the estimated energy by less than −0.001 kcal/mol, suggesting that a stable conformation had been approached.

Site-Directed Mutagenesis. Amino acid substitutions were introduced into plasmid pLD1, which carries the *LeuB* encoding *T. thermophilus* IMDH inserted into pEMBL18$^-$ (26), by site-directed mutagenesis. *E. coli* strain CJ236 and M13K07 helper phage were used to generate uridine-labeled template. Oligonucleotide primers with the necessary mismatches were synthesized on a Biosearch model 8700 DNA synthesizer and used to introduce substitutions into *LeuB* by the method of

The publication costs of this article were defrayed in part by page charge payment. This article must therefore be hereby marked "*advertisement*" in accordance with 18 U.S.C. §1734 solely to indicate this fact.

Abbreviations: IDH, isocitrate dehydrogenase; IMDH, isopropylmalate dehydrogenase.

Table 1. Kinetic parameters of wild-type and mutant enzymes toward NADP and NAD

Enzyme		NADP K_m, μM	NADP k_{cat}, sec^{-1}	NADP k_{cat}/K_m, $\mu M^{-1} \cdot sec^{-1}$	NAD K_m, μM	NAD k_{cat}, sec^{-1}	NAD Performance k_{cat}/K_m, $\mu M^{-1} \cdot sec^{-1}$	Preference NADP performance/ NAD performance
T. thermophilus IMDH								
2 2 2 3 3 2								
2 7 7 2 3 8								
6 8 9 4 β-turn 2 5								
S D I PPDLGGS------AG A	(Wild type)	1750	0.26	1.5×10^{-4}	12	0.15	1.3×10^{-2}	1.2×10^{-2}
R - - ---------- -	(Mutant I)	722	0.88	1.2×10^{-3}	31	0.48	1.5×10^{-2}	8.0×10^{-2}
R K Y ---------- -	(Mutant II)	14	0.09	6.4×10^{-3}	1,836	1.91	1.0×10^{-3}	6.4
R K Y TYDLERLADGAKLAG -	(Mutant III)	25	0.59	2.3×10^{-2}	17,800	1.90	1.1×10^{-4}	2.1×10^{2}
R K Y TYDLERLADGAKLAG V	(Mutant IV)	20	0.39	2.0×10^{-2}	25,560	0.52	2.0×10^{-5}	1.0×10^{3}
E. coli IDH (5)								
2 3 3 3 4 3 2 3								
9 4 4 9 0 5 0 3								
2 4 5 0 α-helix and loop 4 3 2 3								
R K Y TYDFERLMDGAKLLK V C C	(Wild type)	17	80.5	4.7	4,700	3.2	7.0×10^{-4}	6.9×10^{3}
- D I -K---S--------- A I Y	(NAD-IDH)	5800	4.7	8.1×10^{-4}	99	16.2	1.6×10^{-1}	5.0×10^{-3}

Residues in IMDH are numbered vertically and according to the *T. thermophilus* sequence (9) and residues in IDH are numbered according to the *E. coli* sequence (10). Amino acids are denoted by the single-letter code with dashes representing an absence of mutation. All apparent standard errors are <15% of the estimates.

Kunkel (27). Putative mutants were screened by dideoxy sequencing (28).

Engineering Secondary Structures. PCR overlap extension (29) was used to replace the β-turn of IMDH by an α-helix and loop, modeled on that of *E. coli* IDH, but containing three additional amino acids substitutions. Primers I and III are complementary to alternate strands at either end of the IMDH gene. Primers II and IV, are complementary to each other. Each contains the sequence encoding the modified secondary structure of IDH and a sequence complementary to one side of the β-turn of IMDH. Two fragments, 1.1 kb and 177 bp, were generated with primers I and II or II and IV in separate PCR reactions from the DNA of IMDH mutant RKY. The two fragments were purified, mixed, denatured, and reannealed. Strands having matching sequences at their 3′ ends overlap and act as primers for each other to produce the fusion gene. The recombinant fragment was then amplified using primers I and II. The resulting 1.2-kb hybrid fragment was purified, digested with *Kpn*I and *Sal*I and inserted into the expression vector pEMBL18$^-$. The *Nco*I–*Hin*dIII fragment of 3′-terminal 500 bp of IMDH, which includes the RKY substitutions and the engineered secondary structure, was subcloned into wild-type IMDH and sequenced.

Cell Growth and Enzyme Purification. Mutated plasmids were transformed into *E. coli* strain C600 (which is *LeuB*$^-$) and

Table 2. Aligned primary sequences surrounding the coenzyme binding pocket of the decarboxylating dehydrogenases

Enzyme	Sequence		
NAD-dependent IMDH	217 226	268 278 285	323 336
Acremonium chrysogenum	**D**SMAMLMVRD**P**RRF	IY**E**PVH**GSAP**DISGKGLA**NP**VAQIL**S**	RTG**D**LGGR-------ATCSQV
Bacillus subtilis	**D**SAAMQLIYA**P**NQF	LF**E**PVH**GSAP**DIAGKGMA**NP**FAAIL**S**	RTR**D**LARS----EEFSSTQAI
Candida utilis	**D**SAAMILIKY**P**TQL	LY**E**PCH**GSAP**DL-PANKV**NP**IATIL**S**	RTG**D**LKGT-------NSTTEV
Escherichia coli	**D**NATMQLIKD**P**SQF	LY**E**PAG**GSAP**DIAGKNIA**NP**IAQIL**S**	RTG**D**LARG----AAAVSTDEM
Saccharomyces cerevisiae	**D**SAAMILVKN**P**THL	LY**E**PCH**GSAP**DL-PKNKV**DP**IATIL**S**	RTG**D**LGGS-------NSTTEV
Thiobacillus ferrooxidans	**D**NAAMQLIRA**P**AQF	MY**E**PIH**GSAP**DIAGQDKA**NP**LATIL**S**	RTA**D**IAAP-------GTPVIG
Thermus thermophilus	**D**AMAMHLVRS**P**ARF	VF**E**PVH**GSAP**DIAGKGIA**NP**TAAIL**S**	PPP**D**LGGS-------AGTEAF
Yarrowia lipolitica	**D**SAAMILIKQ**P**SKM	LY**E**PCH**GSAP**DL-GKQKV**NP**IATIL**S**	TTA**D**IGGS-------SSTSEV
NAD-dependent TDH			
Pseudomonas putida	**D**ILCARFVLQ**P**ERF	LF**E**PVH**GSAP**DIFGKNIA**NP**IAMIW**S**	VTP**D**MGGT-------LSTQQV
NAP-dependent IDH			
Bos taurus	**D**TVCLNMVQD**P**SQF	IF**E**SVH**GTAP**DIAGKDMA**NP**TALLL**S**	LTK**D**LGGN-------SKCSDF
Homo sapiens	**D**TVCLNMVQD**P**SQF	IF**E**SVH**GTAP**DIAGKDMA**NP**TALLL**S**	LTK**D**LGGN-------AKCSDF
S. cerevisiae	**D**NSVLKVVTN**P**SAY	IF**E**AVH**GSAP**DIAGQDKA**NP**TALLL**S**	RTG**D**LAGT-------ATTSSF
NADP-dependent IDH	283 292	334 344 351	389 406
Anabaena sp.	**D**SIFQQIQTR**P**DEY	VF**E**ATH**GTAP**KHAGLDRI**NP**GSVIL**S**	VTY**D**LARLLEPPVEPLKCSEF
B, subtilis	**D**IFLQQILTR**P**NEF	IF**E**ATH**GTAP**KYAGLDKV**NP**SSVIL**S**	VTY**DF**ARLMDGATE-VKCSEF
E. coli	**D**AFLQQILLR**P**AEY	LF**E**ATH**GTAP**KYAGQDKV**NP**GSIIL**S**	VTY**DF**ERLMDGAKL-LKCSEF
T. thermophilus	**D**NAAHQLVKP**P**EQF	IF**E**AVH**GSAP**KYAGKNVI**NP**TAVLL**S**	LTG**D**VVGYDRGAKT-TEYTEA
Vibrio sp.	**D**AMLQQVLLR**P**AEY	VF**E**ATH**GTAP**KYAGKNKV**NP**GSVIL**S**	VTY**DF**ERLMDDATL-VSCSAF

Numbering for NAD-dependent enzymes follows *T. thermophilus* IMDH. Numbering for the NADP-dependent enzymes follows *E. coli* IDH. The single-letter amino acid code is used throughout. Boldface type denotes rigidly conserved residues. NAD-dependent IMDH (isopropylmalate dehydrogenase): *A. chrysogenum* (H. Kimura, S. Matumura, M. Suzuki & Y. Sumino, GenBank accession no. D50665), *B. subtilis* (11), *C. utilis* (12), *E. coli* (13), *S. cerevisias* (14), *T. ferrooxidans* (15), *T. thermophilus* (9), and *Y. lipolitica* (16). NAD-dependent tartrate dehydrogenase (TDH) of *P. putida* (17). Catalytic subunit of the mitochondrial NAD-dependent eukaryotic IDH: *B. taurus* (18), *H. sapiens* (19), and *S. cerevisiae* (20). NADP-dependent eubacterial IDH (isocitrate dehydrogenase): *Anabaena* sp. (21), *B. subtilis* (22), *E. coli* (10), *T. thermophilus* (23), and *Vibrio* sp. (24).

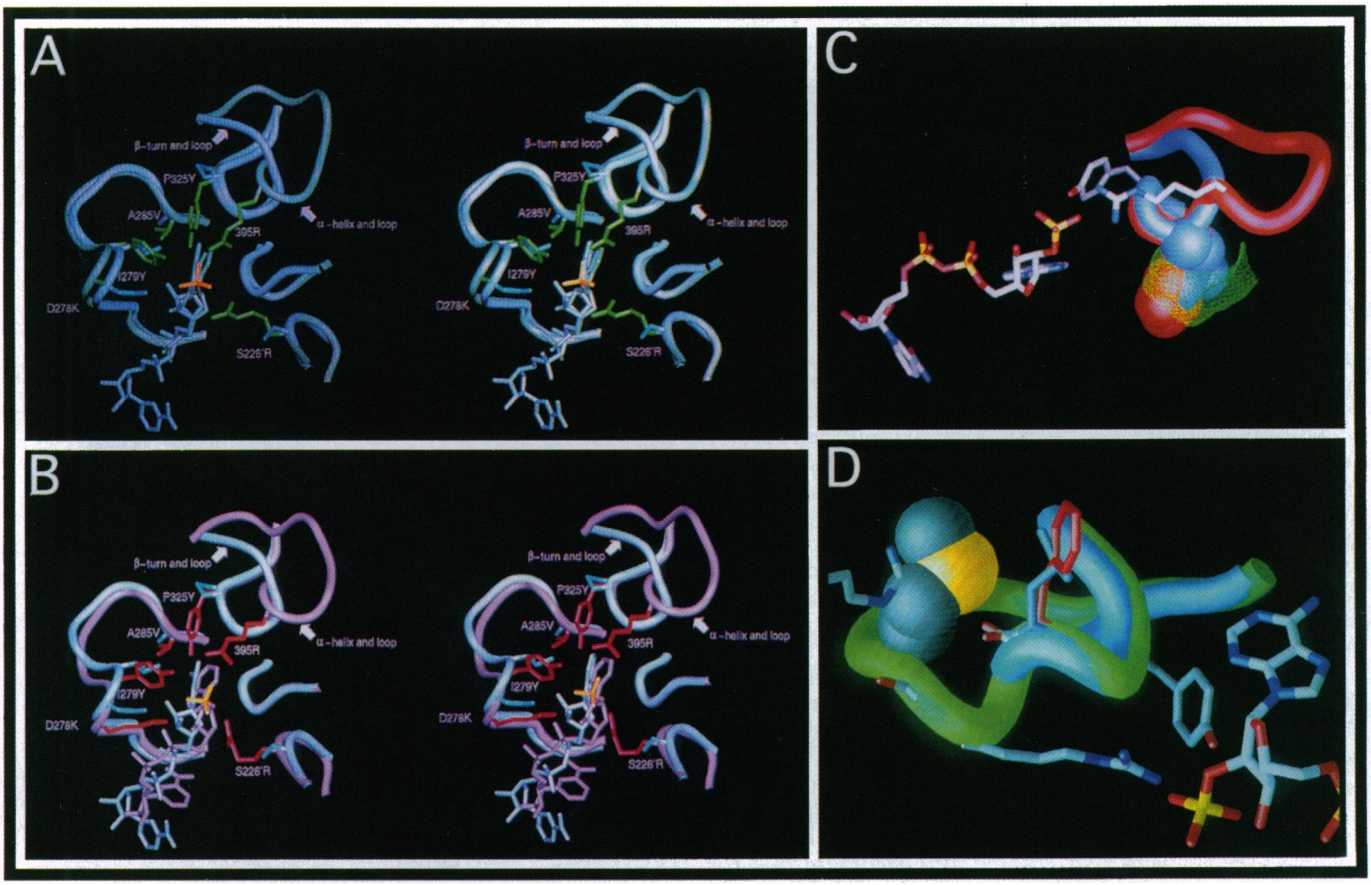

FIG. 1. (*A*) Stereoview of a superposition of the IMDH binary complex with NAD (light blue with side chains in dark blue) on the IDH binary complex with NADP (light green with dark green side chains and the 2′-phosphate of NADP in yellow). IMDH numbering is used throughout, except in the α-helix and loop of IDH, where IDH numbering is italicized. Asp-278 is a major determinant in IMDH, forming a double H-bond with the 2′- and 3′-hydroxyls of the adenosine ribose of NAD. Specificity toward NADP is conferred by four residues in IDH (Arg-226′, Tyr-279, Tyr-325, and *395-Arg*), which form H-bonds to the 2′-phosphate. Two residues emanate from the α-helix, which replaces the β-turn of IMDH. A fifth, Lys-278, is disordered. (*B*) Stereoview of an energy-minimized model of the engineered NADP-dependent enzyme (pink with side chains in red and the 2′-phosphate of NADP in yellow) superposed on that of wild-type IMDH. The overall secondary structure is similar to that of wild-type IDH. The NADP adopts a position reminiscent of that seen in wild-type IDH, with the 2′-phosphate making similar interactions with surrounding side chains. Lys-278 interacts with the 2′-phosphate and 3′-OH of NADP, but additional modelling reveals that it can just as easily interact with the phosphate backbone of NADP. (*C*) Superposition of the IMDH β-turn (blue) on the IDH α-helix and loop (red) showing that the side chain of Phe-327 in IDH (red spheres) is too large to be satisfactorily accommodated in the IMDH pocket (green mesh). Substituting leucine (blue spheres) found in IMDH fills the pocket, thus preventing disruptions in the α-helix and the interactions between Tyr-325 and *395-Arg* and the 2′-phosphate of NADP. (*D*) Superposition of the IDH α-helix and loop (green) on the IMDH β-turn (blue). *Met-397* (solid spheres) in an IDH-like α-helix and loop blocks Arg-115 forming H-bonds with the main chain carbonyls of residues 327 and *396*, potentially destabilizing this region. Substituting alanine at this site allows the interactions to be retained.

grown to full density overnight in 1 liter of Luria broth at 37°C in the presence of 60 μg/ml of ampicillin. Enzymes were purified by the method of Yamada *et al.* (30) with minor modifications (26). Briefly, sonicated extracts were incubated at 75°C for 20 min and the denatured proteins removed by centrifugation. Following removal of nucleic acids with spermidine sulfate, the supernatant was subjected to DEAE anion chromatography, and then further purified and concentrated by ammonium sulfate precipitation. The final mutant, unlike the wild-type enzyme, binds tightly to Affi-Gel blue. This provides an additional means to purify the mutant by affinity chromatography. As judged by Coomassie blue staining after SDS/PAGE electrophoresis, all preparations were at least 95% free from contaminating protein.

Kinetic Analyses. The buffer used contained 100 mM KCl, 1 mM DTT, 25 mM Mops (pH 7.3) at 21°C, with 200 μM isopropylmalate or 1 mM isocitrate and 5 mM free Mg^{2+} added as $MgCl_2$, the quantity determined by the Mg^{2+}-substrate and Mg^{2+}-coenzyme dissociation constants (31). Kinetic parameters were determined by following the reduction of the nicotinamide coenzymes at 340 nm in 10-mm cuvettes mounted in a Hewlett–Packard model 8452 single-beam diode array spectrophotometer. Rates were calculated using a molar extinction coefficient for NAD(P)H of 6,200 $M^{-1}\cdot cm^{-1}$ and protein concentrations were determined at 280 nm using a molar extinction coefficient of 30,420 $M^{-1}\cdot cm^{-1}$ (30). Nonlinear least-squares Gauss–Newton regressions were used to determine the fit of the data to the Michaelis–Menten model.

RESULTS

Molecular Modeling. In an energy-minimized model of the engineered coenzyme binding pocket (Fig. 1*B*), the Cαs in the introduced α-helix (which contains substitutions Pro-324-Thr, Phe-327-Leu and *Met-397-Ala* that are necessary to avoid steric effects disrupting local secondary structures) remain within 0.2 Å of those in IDH. However, the terminal loop shifts noticeably, there being no constraints forcing it to remain in precisely the same conformation seen in IDH. The position of residues Asp-278-Lys and Ile-279-Tyr in the 277–286 loop remain similar to those in IMDH, rather than shifting approximately 1 Å to the left as in IDH. Nevertheless, the overall secondary

structure of the model is very similar to wild-type IDH, suggesting that an engineered mutant should be stable and functional.

The NADP in the model shifts to a position reminiscent of that seen in wild-type IDH (Fig. 1*B*). The H-bond between the N2 of the adenine ring and main chain amide of residue 286 is disrupted, and the sugar pucker changes from 3′C to 2′C endo. Interactions between the 2′-phosphate of NADP and Ser-226′-Arg, Ile-279-Tyr, and Pro-325-Tyr and *395-Arg* in the α-helix, mimic those seen in wild-type IDH. The conformational flexibility of Asp-278-Lys also allows it to interact with the phosphate backbone of the dinucleotide, as well as with the 2′-phosphate and 3′-OH of NADP as visualized (Fig. 1*B*). The modeled interactions are sufficiently similar to those of IDH as to suggest that changing coenzyme specificity by engineering secondary structures is feasible.

Site-Directed Mutagenesis. Site-directed mutagenesis was used to replace Ser-226′, which is located in a loop on the second subunit of IMDH, by Arg. As expected, the Ser-226′-Arg substitution has little effect on performance (k_{cat}/K_m) with NAD (Table 1, mutant I). In contrast, performance with NADP improves 8-fold, a result consonant with formation of an ionic H-bond with the 2′-phosphate of NADP and/or a general increase in the electrostatic potential in the coenzyme binding pocket.

Asp-278 and Ile-279 lie in a loop on the left side of the nucleotide binding pocket (Fig. 1 *A* and *B*). Replacing Asp-278 by Lys disrupts the H-bonds critical to NAD specificity and eliminates any possible electrostatic repulsion of NADP. Substituting Ile-279 by Tyr should maintain a hydrophobic interaction with the adenine, while permitting an H-bond to form the 2′-phosphate of NADP. As expected from the loss of the double H-bonds with Asp-278, the affinity toward NAD is dramatically reduced: the K_m increases from 31 μM to 1836 μM (Table 1, mutant II). By contrast, the gain of two units of electrostatic potential and H-bonds causes a dramatic improvement in affinity toward NADP: the K_m decreases from 722 μM to 14 μM. Interestingly, whereas the k_{cat} with NAD increases 4-fold, the k_{cat} with NADP decreases 10-fold. Perhaps NADP binds in a nonproductive manner in the triple RKY mutant. Preference now favors NADP over NAD only by a modest factor of six (Fig. 2).

Engineering a Secondary Structure. Pro-325 participates in the formation of a β-turn on the right side of the nucleotide binding pocket (Fig. 1*A*). In IDH this residue is replaced by Tyr, which occupies a similar position, yet resides in an α-helix. The Tyr interacts with the 2′-phosphate of NADP, while its bulk pushes the adenine ring toward the right side of the nucleotide binding pocket. Such a shift should weaken the H-bond formed between the adenine N2 and the main chain amide of residue 286: in IMDH the 2.9-Å H-bond is perpendicular to the N2 and lifted 20° from the plane of the adenine ring (6), whereas in IDH the 3.2-Å H-bond is 30° from perpendicular and lifted 50° from the plane (2). However, any loss of affinity toward the coenzymes might be compensated in the case of NADP by a newly established H-bond between 2′-phosphate and Pro-325-Tyr. Further along the IDH α-helix is *395-Arg* (Table 1, IDH numbering), which has no equivalent in the β-turn of IMDH. *395-Arg* also H-bonds to the 2′-phosphate of NADP (Fig. 1). Introduction of this Arg in IMDH is expected to further impair NAD binding by increasing the polarity of the nucleotide binding pocket and improve affinity for NADP through the addition of an ionic H-bond to the 2′-phosphate. Hence, improving specificity toward NADP requires that the secondary structure of IMDH must be engineered from a β-turn to an α-helix and loop.

Engineering an α-helix and loop into IMDH requires more than merely exchanging the secondary structures found in IDH, because modeling indicates that it is incompatible with the remaining IMDH structure. The modifications introduced

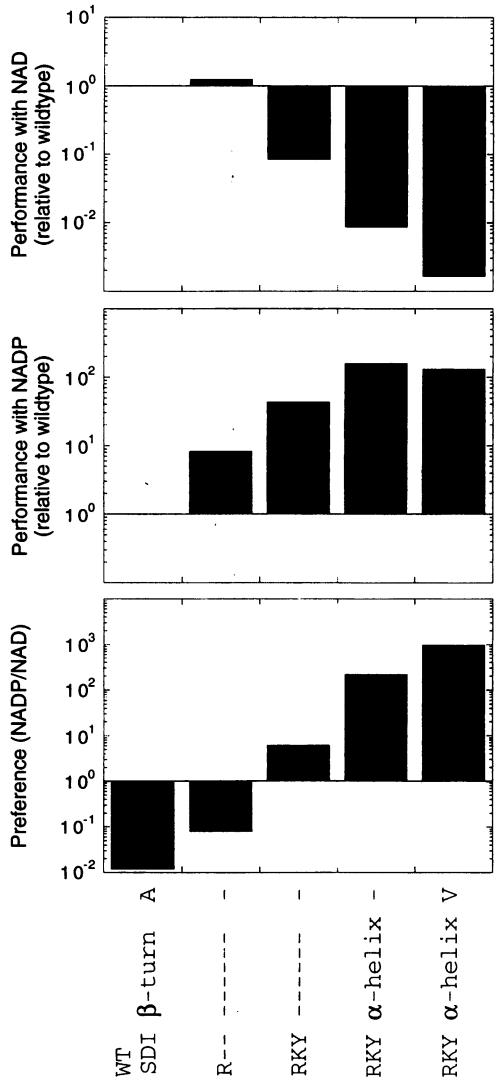

FIG. 2. The systematic shift in coenzyme preference generated by engineering mutants of IMDH. The height of the columns represents the degree to which performance (k_{cat}/K_m) and preference [$(k_{cat}/K_m)_{NADP}/(k_{cat}/K_m)_{NAD}$] is improved or impaired.

are as follows (Table 1, mutant III). The rigid Pro-324 just proximal to the helix is replaced by the more conformationally flexible threonine, found in related sequences (Table 2), to allow minor shifts in the peptide backbone that might enable the tyrosine substituted for Pro-325 to better interact with the 2′-phosphate of NADP. Rather than substituting phenylalanine, the Leu-327 of IMDH (Table 2) is retained to avoid the steric crowding that would otherwise perturb the α-helix and disrupt interactions with NADP (Fig. 1*C*). The *397-Met* of IDH (Table 1, IDH numbering) is replaced by alanine, again to avoid steric crowding (Fig. 1*D*) and to preserve an H-bond between Arg-115 and the main chain carbonyls at residues 327 (IMDH numbering) and *396* (IDH numbering). The final two amino acids at the terminus of the IMDH β-turn, Ala-332 and Gly-333, were retained to avoid steric packing problems associated with substituting the leucine and lysine of IDH.

The resulting engineered RKY mutant enzyme with its IDH-like α-helix and loop is stable and active at 75°C for 30 min, suggesting that the tertiary structure is folded correctly. Kinetic analysis reveals that the K_m toward NAD increases 10-fold, that the K_m toward NADP increases 2-fold, but so does k_{cat}, by a factor of six. These results are consonant with the notion that the H-bond between the adenine N2 and the main chain amide at site 286 is disturbed and, in the case of NADP,

compensated by H-bonds to the 2′-phosphate of NADP. Overall, engineering the secondary structure increases the preference for NADP by a factor of 35–208 (Table 1, Fig. 2).

A Final Substitution. Ala-285, which lies at the back of the nucleotide binding pocket, makes no direct contact with the bound coenzymes. However, molecular modeling suggests that substituting the valine found in IDH will, with its bulkier side chain, force the adenine ring to shift, further disrupting the H-bond between the adenine N2 and the main chain amide at residue 286. The resulting loss in affinity might be compensated in the case of NADP by improved interactions between the 2′-phosphate and the introduced Asp-278-Lys, Ile-279-Tyr, Pro-325-Tyr, and *395-Arg*. Indeed, whereas performance of the final mutant with NAD is impaired by a factor of 5, the performance with NADP is largely maintained. Preference now favors NADP over NAD by a factor of 1000 (Table 1, mutant IV; Fig. 2). Like wild-type IDH, and unlike wild-type IMDH, this final mutant binds tightly to Affi-Gel blue affinity columns. This provides additional evidence to support the notion that an IDH-like NADP binding pocket has been successfully engineered.

DISCUSSION

Replacing the seven residues of a β-turn in *T. thermophilus* IMDH by a 13-residue sequence modeled on an α-helix and loop in *E. coli* IDH, together with four additional substitutions, cause a dramatic shift in preference from NAD to NADP by a factor 100,000, without significantly affecting performance (Table 1, mutant IV; Fig. 2). An energy-minimized model suggests that the engineered secondary structures are stable (Fig. 1*B*), a notion confirmed by the fact that the final mutant enzyme remains active at 75°C. Furthermore, like NADP-dependent IDH and unlike the wild-type NAD-dependent IMDH, the engineered mutant binds to Affi-Gel blue affinity chromatography resin. These results suggest that rational engineering of secondary structures to produce enzymes with novel properties is feasible.

Problems with Homology Engineering. Difficulties in identifying key specificity determinants, particularly when comparing highly divergent enzymes where one or more crystallographic structures are absent, probably accounts for the many failed attempts to invert specificities. For example, an early attempt to engineer coenzyme specificity in IMDH failed to identify Asp-278 as a critical determinant of specificity on the grounds that it was too far from the bound coenzyme in IDH (32)—the realization that the positions of the bound coenzymes differed required the determination of the structure of the binary coenzyme–IMDH complex for comparison with that of IDH (6).

Another example is the Ala-285-Val substitution. In the current model, a valine methyl occupies the same position as the Cβ of alanine, packing against the hydrophobic core. This forces the valinel Cβ to move, causing a local conformational change in the peptide backbone and nudging the adenine ring of NADP (Fig. 1 *A* and *B*). The shift in the position of the adenine ring disrupts the H-bond formed between its N2 and the main chain amide at 286, thereby weakening coenzyme binding. This scenario is entirely consistent with the recently determined structure of the engineered NAD-dependent *E. coli* IDH (32), which reveals that the opposite substitution, Val-285-Ala, mirrors the effects modeled here: the introduced alanine allows the peptide backbone of IDH to relax so that the adenosine shifts back into a position where its N2 establishes an H-bond with the main chain amide of residue 286. This in turn allows the ribose of NAD to approach the aspartic acid introduced at site 278 and establish the H-bonds so critical to specificity (6, 33). The importance of site 285 to specificity would, in all likelihood, have remained unnoticed in the absence of the structure of either binary complex.

Additional problems arise when sequence homology is used as a criterion, rather than as a guide, for introducing substitutions. Sequence alignments alone suggest that substitutions Pro-325-Tyr and Gly-329-Arg (equivalent to *395-Arg* in IDH) are needed to convert IMDH to an NADP utilizing enzyme. But without engineering local secondary structures, these substitutions would undoubtedly disrupt the β-turn, causing loss of function. The reverse attempt would suggest replacing the 325-Tyr and *395-Arg* in the α-helix of IDH by glycine. However, their flexibility destabilizes this region leading to a marked reduction in performance (33). Sequence homologies would also miss site 285 as being important—several NAD-dependent IMDHs already have a valine at this site, no doubt because of local packing differences. Finally, consideration of sequence homologies alone may sometimes lead to substituting rigidly conserved amino acids, which have nothing to do with specificity *per se* and everything to do with an alternate means to stabilized similar secondary structures (5, 32). The resulting mix is disruptive.

Determinants of Coenzyme Specificity. The complete inversion of coenzyme specificities in both IMDH (Fig. 2) and IDH (5) demonstrates that coenzyme specificities in the β-decarboxylating dehydrogenases are principally determined by interactions between the nucleotides and surface amino acid residues lining the binding pockets. Nevertheless, additional residues not in contact with the coenzymes play key roles through indirect effects. Two obvious examples are the Phe-327-Leu and Met-397-Ala substitutions in the introduced α-helix and loop, which allow these secondary structures to pack correctly against the IMDH core. Less obvious, perhaps, are Ala-285 in IMDH and the Pro-324-Thr substitution, which allows the position of the Cα of Pro-325-Tyr in the engineered α-helix to adjust, thereby facilitating H-bond formation between the relatively rigid tyrosine side chain and the 2′-phosphate of NADP. These studies demonstrate that protein engineering provides a powerful tool to fully elucidate the mechanisms determining specificity.

We thank Ken Neet for his thoughtful suggestions. This work was supported by U.S. Public Health Service Grant GM-48735 from the National Institutes of Health.

1. Rossmann, M. G., Moras, D. & Olsen, K. W. (1974) *Nature (London)* **250,** 194–199.
2. Hurley, J. H., Dean, A. M., Koshland, D. E., Jr. & Stroud, R. M. (1991) *Biochemistry* **30,** 8671–8678.
3. Bocanegra, J. A., Scrutton, N. S. & Perham, R. N. (1993) *Biochemistry* **32,** 2737–2740.
4. Nishiyama, M., Birktoff, J. J. & Beppu, T. (1993) *J. Biol. Chem.* **268,** 4656–4660.
5. Chen, R., Greer, A. & Dean, A. M. (1995) *Proc. Natl. Acad. Sci. USA* **92,** 11666–11670.
6. Hurley, J. H. & Dean, A. M. (1994) *Structure* **2,** 1007–1016.
7. Hurley, J. H., Thorsness, P., Ramalingham, V., Helmers, N., Koshland, D. E., Jr., & Stroud, R. M. (1989) *Proc. Natl. Acad. Sci. USA* **86,** 8635–8639.
8. Imada, K., Sato, M., Tanaka, N., Katsube, Y., Matsuura, Y. & Oshima, T. (1991) *J. Mol. Biol.* **222,** 725–738.
9. Tanaka, T., Kwano, N. & Oshima, T. (1981) *J. Biochem. (Tokyo)* **89,** 677–682.
10. Thorsness, P. E. & Koshland, D. E., Jr. (1987) *J. Biol. Chem.* **262,** 10422–10425.
11. Imai, R., Sekiguchi, T., Nosoh, Y. & Tsuda, K. (1987) *Nucleic Acids Res.* **15,** 4988.
12. Hamasawa, K., Kobayashi, Y., Harada, S., Yoda, K., Yamasaki, M. & Tamura, G. (1987) *J. Gen. Microbiol.* **133,** 1089–1097.
13. Kirino, H., Aoki, M., Aoshima, M., Hayashi, Y., Ohba, M., Yamagishi, A., Wakagi, T. & Oshima, T. (1994) *Eur. J. Biochem.* **229,** 275–281.
14. Andreadis, A., Hsu, Y. P., Hermodgon, M., Kohlhaw, G. & Schimmel, P. (1984) *J. Biol. Chem.* **259,** 8059–8062.
15. Kawaguchi, H., Inagaki, K., Kuwata, Y., Tanaka, H. & Tano, T. (1993) *J. Biochem. (Tokyo)* **114,** 370–377.

16. Davidow, L. S., Kaczmarek, F. S., Dezeeuw, J. R., Conlon, S. W., Lauth, M. R., Pereira, D. A. & Franke, A. E. (1987) *Curr. Genet.* **11,** 377–383.
17. Tipton, P. A. & Beecher, B. S. (1994) *Arch. Biochem. Biophys.* **313,** 15–21.
18. Zeng, Y., Weiss, C., Yao, T. T., Huang, J., Siconolfi-Baez, L. & Hsu, P. (1995) *Biochem. J.* **310,** 507–516.
19. Kim, Y. O., Oh, I. U., Park, H. S., Jeng, J., Song, B. J. & Huh, T. L. (1995) *Biochem. J.* **308,** 63–68.
20. Cupp, J. R. & McAlister-Henn, L. (1993) *Biochemistry* **32,** 9323–9328.
21. Muro-Pastor, M. I. & Florencio, F. J. (1994) *J. Bacteriol.* **176,** 2718–2726.
22. Jin, S. & Sonenshein, A. L. (1994) *J. Bacteriol.* **176,** 4669–4679.
23. Miyazaki, K., Eguchi, H., Yamagishi, A., Wakagi, T. & Oshima, T. (1992) *Appl. Environ. Microbiol.* **58,** 93–98.
24. Ishii, A., Suzuki, M., Sahara, T., Takada, Y., Sasaki, S. & Fukunaga, N. (1993) *J. Bacteriol.* **175,** 6873–6880.
25. Bolduc, J. M., Dyer, D. H., Scott, W. G., Singer, P., Sweet, R. M., Koshland, D. E., Jr., & Stoddard, B. L. (1995) *Science* **268,** 1312–1318.
26. Dean, A. M. & Dvorak, L. (1995) *Protein Sci.* **4,** 2156–2167.
27. Kunkel, T. A., Roberts, J. D. & Zakour, R. A. (1987) *Methods Enzymol.* **154,** 367–382.
28. Sanger, F., Nicklen, S. & Coulsen, R. (1977) *Proc. Natl. Acad. Sci. USA* **74,** 5463–5467.
29. Horton, R. M., Hunt, H. D., Ho, S. N., Pullen, J. K. & Pease, L. R. (1989) *Gene* **77,** 61–68.
30. Yamada, T., Akutsu, N., Miazaki, K., Kakinuma, K., Yoshida, M. & Oshima, T. (1990) *J. Biochem. (Tokyo)* **108,** 449–456.
31. Dean, A. M. & Koshland, D. E., Jr. (1993) *Biochemistry* **32,** 9302–9309.
32. Miyazaki, K. & Oshima, T. (1994) *Protein Eng.* **7,** 401–403.
33. Hurley, J. H., Chen, R. & Dean, A. M. (1996) *Biochemistry*, in press.